X-ray and electrostatic levitation undercooling studies in Ti–Zr–Ni quasicrystal forming alloys

K.F. Kelton [a,*], A.K. Gangopadhyay [a], G.W. Lee [a], L. Hannet [b],
Robert W. Hyers [c], S. Krishnan [d], Michael B. Robinson [c], Jan Rogers [c],
Thomas J. Rathz [c]

[a] *Department of Physics, Campus Box 1105, Washington University, One Brookings Drive, St. Louis, MO 63130-4899, USA*
[b] *CNRS-CRMHT, Orleans cedex 2, France*
[c] *NASA Marshall Space Flight Center, Mail Code SD47, Huntsville, AL 35812, USA*
[d] *KLA-Tencor Film and Surface Technology, 160 Rio Robles, San Jose, CA 95134, USA*

Abstract

The first undercooling measurements on electrostatic-levitated droplets of TiZrNi alloys that form the icosahedral quasicrystal phase are presented. The reduced undercooling for crystallization decreases with an increasing polytetrahedral order of the primary solidifying phase, suggesting the development of icosahedral short-range order in the undercooled liquid. X-ray diffraction measurements made at the advanced photon source on liquid droplets of these alloys, aerodynamically levitated and heated to near their liquidus temperature, however, show only weak evidence for increased icosahedral order. This suggests that significant ordering occurs below the melting temperature.
© 2002 Elsevier Science B.V. All rights reserved.

1. Introduction

To explain the ability of many liquids to persist for a significant time below their melting temperature [1], Frank proposed that the local atomic structures of these undercooled liquids are icosahedral [2]. This can be investigated by studying the nucleation and growth of icosahedral quasicrystals (i-phase), condensed phases that show extended icosahedral order. In this report, we present the first undercooling studies of electrostatic-levitated liquids that form the TiZrNi i-phase. These stable quasicrystals [3] may be useful in hydrogen storage and battery applications [4]. Initial results from X-ray diffraction studies of levitated TiZrNi liquids near their melting temperatures are also presented.

2. Experimental procedure

Ingots of TiZrNi were prepared by arc-melting on a water-cooled Cu hearth under high-purity argon gas. The small samples (2.3–2.5 mm in diameter) required for the electrostatic levitation

---

* Corresponding author. Tel.: +1-314 935 6228; fax: +1-314 935 6219.

E-mail address: kfk@wuphys.wustl.edu (K.F. Kelton).

(ESL) experiments were prepared by cracking the large ingots and re-melting small pieces. Those samples were subsequently levitated in vacuum ($\approx 10^{-7}$ Torr) between two electrostatic plates and heated by a YAG laser in an ESL facility, located at NASA/Marshall Space Flight Center [5]. Microstructure and phase information were obtained on as-cast and ESL-processed samples by powder X-ray diffraction, and by transmission electron microscopy (TEM) and scanning electron microscopy (SEM), both equipped for energy dispersive X-ray spectroscopy studies of phase composition.

X-ray diffraction measurements were made on beamline 12-1D-B of the advanced photon source. A beam energy of 17 keV was used to avoid fluorescence from the Zr K-edge. Specimens were aerodynamically levitated and positioned with respect to the incident X-ray beam in the conical nozzle levitation apparatus using ultra-high-purity argon gas [6]. Laser heating was used to melt and control the temperature of the sample, which was measured with an optical pyrometer operating at a wavelength of 650 nm, assuming a sample emissivity of 0.35.

The scattered X-ray intensity was measured using a solid-state detector with a 350 eV resolution for $2° \leqslant 2\theta \leqslant 110°$, corresponding to $0.5 \leqslant Q \leqslant 15$ Å^{-1}. The raw data were corrected for detector dead time, beam energy profile, and specimen geometry to extract the X-ray weighted average structure factor, $S(Q)$ [7].

3. Results and discussion

A cut of the TiZrNi phase diagram for equal Ti and Zr concentrations is shown in Fig. 1. The high temperature solid solution phase, β-Ti/Zr (bcc with $a = 3.3$ Å for pure Ti), is the primary solidification phase for alloys made with a low Ni concentration. Liquidus temperatures measured in ESL and solidification microstructures reveal a eutectic at [Ni] ≈ 21 at.%. For higher Ni concentrations, the polytetrahedral C14 Laves phase (cph, $a = 5.29$ Å and $c = 8.42$ Å) is the primary solidification phase. The i-phase is stable at low temperatures near ≈ 17 at.% Ni, formed by a solid-
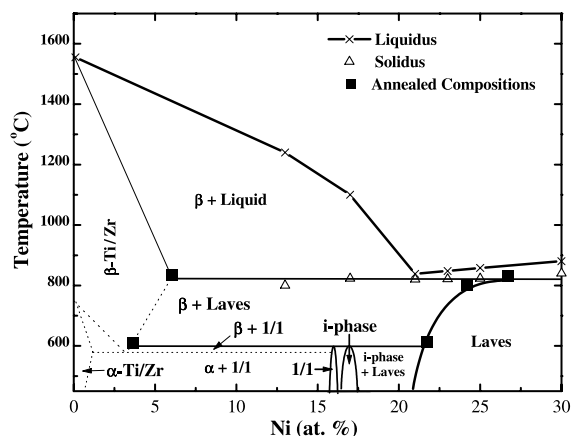

Fig. 1. Schematic vertical section of TiZrNi phase diagram along a line of equal Ti and Zr, showing the phases that form in equilibrium.

state transformation from the α-Ti/Zr and the C14 phases at ≈ 570 °C [4].

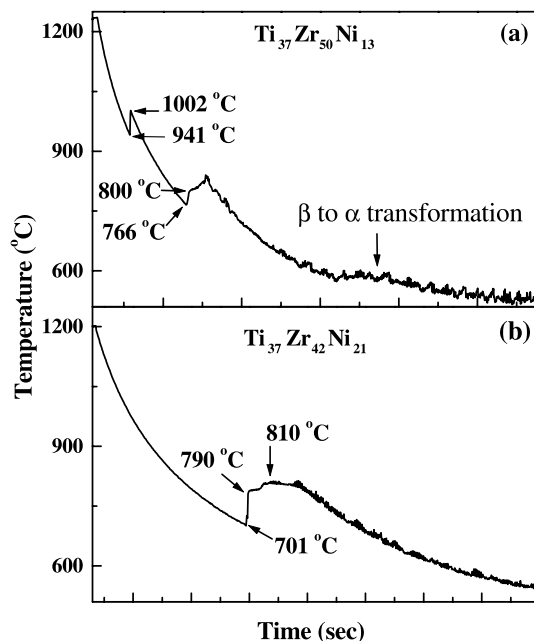Fig. 2(a) shows the measured sample temperature for the free radiation cooling of an electro-

Fig. 2. Cooling curves for electrostatic-levitated liquid 3 mm droplets of (a) $Ti_{37}Zr_{50}Ni_{13}$ and (b) $Ti_{37}Zr_{42}Ni_{21}$; the recalescence temperatures are indicated.

static-levitated 3 mm diameter liquid droplet of $Ti_{37}Zr_{50}Ni_{13}$. The temperature rise (recalescence) at 941 °C is due to the heat evolved during transformation to a phase mixture of β-Ti/Zr and the liquid phase. The lower temperature recalescence is due to the solidification of the remaining liquid to the C14 phase. The feature at 800 °C is due to an emissivity change with surface crystallization. Fig. 2(b) shows the cooling curve for a droplet of $Ti_{37}Zr_{42}Ni_{21}$. Recent studies of rapidly solidified droplets at this composition indicate that the recalescence at 700 °C corresponds to the nucleation and growth of the icosahedral phase [8]. Because the equilibrium phase field for the i-phase does not extend to the liquidus temperature, however, this is a metastable solidification product. The plateau at 790 °C corresponds to the metastable solidus temperature. The second rise to 810 °C corresponds to the formation of the C14 phase. These results indicate that the local order of the liquid is more similar to that of the icosahedral quasicrystal than to the polytetrahedral C14 phase.

The reduced undercooling is defined as $\Delta T_r = (T_m - T_c)/T_m$, where T_c is the temperature of crystallization and T_m is the melting temperature (in K). For a known driving free energy, ΔT_r provides a measure of the interfacial free energy [1,9]. The values obtained for the three phases studied are: i-phase, $\Delta T_r = 0.11 \pm 0.015$; C14 phase, $\Delta T_r = 0.15 \pm 0.01$; α(Ti/Zr), $\Delta T_r = 0.19 \pm 0.01$. The error bars reflect the uncertainty in the measured liquidus temperatures. These results are consistent with those from electromagnetic levitation (EML) studies of Al-based alloys [9]; the relative undercooling increases as the structure of the crystal becomes less tetrahedral, signaling an increasing interfacial free energy with the liquid phase.

The $S(Q)$ results for the three compositions studied at temperatures close to their liquidus temperatures are shown in Fig. 3. The ability of this method to make structural measurements on levitated reactive metal alloys is evidenced by the high quality of the data. $S(Q)$ is characterized by three distinct peaks. Based on the classification method originally proposed by Price et al. [7], the primary peak in $S(Q)$ corresponds to the topological short-range order typical of most metallic
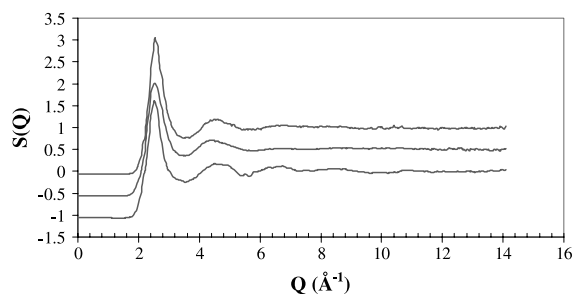

Fig. 3. $S(Q)$ for liquid alloys near their liquidus temperatures for: $Ti_{43}Zr_{43}Ni_{14}$ – lower curve; $Ti_{41.5}Zr_{41.5}Ni_{17}$ – middle curve; $Ti_{40}Zr_{40}Ni_{20}$ – upper curve. The curves have been displaced for clarity.

liquids. The $S(Q)$ for $Ti_{43}Zr_{43}Ni_{14}$ shows additional structure at higher Q, which may indicate network formation in the glass, although further experiments are required to confirm this. The rapid damping of $S(Q)$ in the high-Q region is typical of hard-sphere liquids. The shoulder on the high-Q side of the second peak in $S(Q)$ for $Ti_{41.5}Zr_{41.5}Ni_{17}$ is consistent with developing icosahedral order, although more detailed modeling is required to confirm this.

Fig. 4 shows the $G(r)$ curves obtained by a Fourier transform of the data in Fig. 3. Four well-defined peaks are observed. The total number of atoms within the first coordination shell (the coordination number, C_n) was estimated by integrating under the first peak, using the known composition and form factors. The values for the peak positions in $S(Q)$ and $G(r)$, and for C_n for the
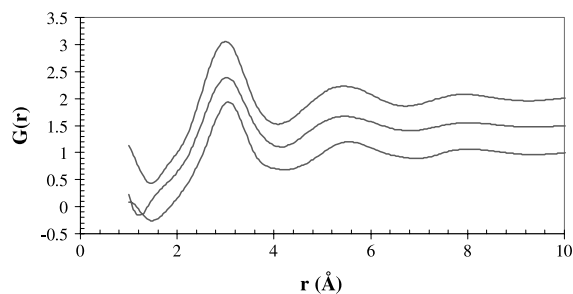

Fig. 4. $G(r)$ for liquid alloys near their liquidus temperatures for: $Ti_{43}Zr_{43}Ni_{14}$ – lower curve; $Ti_{41.5}Zr_{41.5}Ni_{17}$ – middle curve; $Ti_{40}Zr_{40}Ni_{20}$ – upper curve. The curves have been displaced for clarity.

Table 1
Peak positions for $S(Q)$ (Q_1 and Q_2), for $G(R)$ (r_1 and r_2) and the coordination number (C_n) for TiZrNi liquid alloys

Alloy	Q_1 (Å^{-1}) (± 0.02)	Q_2 (Å^{-1}) (± 0.05)	r_1 (Å) (± 0.02)	r_2 (Å) (± 0.03)	r_3 (Å) (± 0.03)	C_n (± 0.5)
$Ti_{43}Zr_{43}Ni_{14}$	2.52	4.50	3.04	5.56	8.0	12.9
$Ti_{41.5}Zr_{41.5}Ni_{17}$	2.52	4.56	3.04	5.44	8.0	12.9
$Ti_{40}Zr_{40}Ni_{20}$	2.55	4.59	3.00	5.44	7.92	12.7

three liquid alloys are summarized in Table 1; the errors were computed following an analysis discussed elsewhere [10]. The first shell in these alloys appears to be dominated by Ti–Zr interactions. As expected, based on the metallic radii of the constituent elements, with increasing nickel concentration, the Ti–Ni and Zr–Ni interactions contribute to the first shell via a reduction in the first-nearest neighbor distance and coordination. The $S(Q)$ and $G(r)$ of these three alloys shows only a gradual change over the range of compositions investigated.

4. Conclusions

The results of the first studies of the undercooling of the TiZrNi icosahedral quasicrystal by ESL are presented. The maximum reduced undercooling for the i-phase ($\Delta T_r \approx 0.1$) is less than for simple crystal phases (typically $\Delta T_r \approx 0.2$), and even less than for the polytetrahedral C14 Laves phase. This is in agreement with earlier EML undercooling studies of Al-based quasicrystal-forming alloys. Significant stirring of the liquid is unavoidable in EML, however; the more quiescent environment possible in ESL opens the door for future studies of the composition dependence of the nucleation, possibly revealing effects of long-range diffusion on the nucleation rate [11]. That X-ray diffraction data from aero-acoustic levitated liquid droplets of these alloys above the liquidus

temperature suggest only weak icosahedral order suggests that it likely develops primarily in the undercooled liquid.

References

[1] K.F. Kelton, in: H. Ehrenreich, D. Turnbull (Eds.), Solid State Physics, vol. 45, Academic Press, 1991, p. 75.
[2] F.C. Frank, Proc. Royal Soc. London 215A (1952) 43.
[3] K.F. Kelton, W.J. Kim, R.M. Stroud, Appl. Phys. Lett. 70 (1997) 3230.
[4] K.F. Kelton, P.C. Gibbons, Mat. Res. Soc. Bull. (1997) 69.
[5] J.R. Rogers, R.W. Hyers, T. Rathz, L. Savage, M.B. Robinson, in: M.S. El-Genk (Ed.), Proceedings of the Space Technology and Applications International Forum 2001, Albequerque, NM, AIP Conf. Proc., vol. 552, 2001.
[6] S. Krishnan, D.L. Price, J. Phys.: Condens. Matter 12 (2000) R145.
[7] D.L. Price, S.C. Moss, R. Reijers, M.-L. Saboungi, S. Sussman, J. Phys. Solid State 21 (1988) L1069.
[8] G.W. Lee, T.K. Croat, A.K. Gangopadhyay, K.F. Kelton, Philos. Mag. Lett. 82 (2002) 199.
[9] D. Holland-Moritz, Int. J. Non-Equilib. Process. 11 (1998) 169.
[10] S. Ansell, S. Krishnan, J.J. Felten, D.L. Price, J. Phys.: Condens. Matter 10 (1998) L73.
[11] K.F. Kelton, Acta Mater. 48 (2000) 1967.